Multi-layered ZnS/CdS Anti–Reflection Coating by Spray Pyrolysis with Nebulizer

[1st] Sawsan H. Abdullah
Research and Technology Center of Environment, Water, and Renewable Energy
Scientific Research Commission
Baghdad, Iraq
sawsanhussein1976@gmail.com

[2nd] Khalil I. Inad
Research and Technology Center of Environment, Water, and Renewable Energy
Scientific Research Commission
Baghdad, Iraq
dr.khalil.inad@gmail.com

[3rd] Ahmed S. Jaber
Information and Communication Technology Research Center
Scientific Research Commission
Baghdad, Iraq
ahmedcctv11@gmail.com

[4th] Salam Waley Shneen*
Energy and Renewable Energies Technology Center
University of Technology
Baghdad, Iraq
salam.w.shneen@uotechnology.edu.iq

*Corresponding author: salam.w.shneen@uotechnology.edu.iq
Received: 2026-03-09; **Accepted:** 2026-07-01

***Abstract*—In this study, zinc sulfide (ZnS) thin films were synthesized using a spray pyrolysis technique. The study targets a multi-layer anti-reflective coating that consists of ZnS and cadmium sulfide (CdS) layers using a modified spray pyrolysis with an ultrasonic atomizer. The aim is to analyze the effect of this coating on the structural and optical properties, notably with regard to transmittance, reflectivity, and Raman analysis. Here, two different thin film layers were deposited with different structure types, which include cubic and hexagonal phases, to achieve the obtained thin films with spray pyrolysis. Multilayer ZnS is described as an effective and inexpensive anti-reflective film that can be used as a solar cell coating. Both phases exist and this is confirmed by X-ray diffraction (XRD) analysis. The average grain size and the surface smoothness of the two-layer films were smaller than those of the other films, whereas the specific surface area was high, as reported by atomic force microscopy (AFM) studies. The CdS/ZnS thin films showed significantly less reflectivity compared to other thin films based on optical measurements using ultraviolet-visible (UV-Vis) spectroscopy and calculated reflectivity from predefined refractive index.**

***Keywords*—Anti-reflecting, Ultrasonic-spray pyrolysis, ZnS, CdS.**

I. INTRODUCTION

An anti-reflection coating involves significantly reducing the reflection from the surface of optical components so that their efficiency is improved by minimizing losses occurring on these surfaces. The structures are made of materials that can be insulating, possessing a low absorption coefficient ($\alpha < 10^3$ cm^{-1}), metallic, or both, and can be designed as thin or multilayer films [1]. Applications of anti-reflection coatings include solar cells and thermal surveying systems, where the properties of the materials utilize these principles. Rayleigh was the first to discuss this phenomenon, concerned mainly with chemical methods [2]. Previously, Michael Faraday performed some of the earliest studies in 1857, making films by passing an electric current through a metallic wire that was then thermally evaporated [3]. Light interference at the same thin-film parallel boundary demonstrates that optical waves propagate within each layer [4]. The light source *S* shines a light beam onto the interface of a thin film at point *A*, which has a thickness *d*, and a portion of that beam reflects into the same medium along ray 1 while another portion of the radiation is transmitted toward *AF*. This is similar to the event at point F, where part of the ray reflects at B, and the remaining light transmits towards H, continuing this pattern until two sets of parallel rays are formed, with intensity diminishing on both sides of the film, as depicted in Fig. 1 [5].

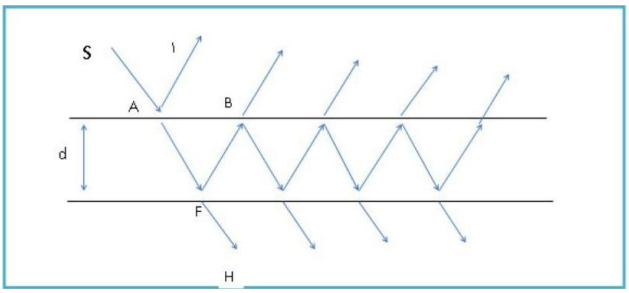

Fig. 1. Thin-film interference process at interfaces with thickness of *d*.

The interaction of light rays can happen in either a destructive or constructive way at the interface that divides the incoming rays from the reflected rays caused by numerous internal reflections within a film of thickness (d). The criteria for both destructive and constructive interference are described in [6]:

$$nd = \delta = \pi/2 \quad (1)$$

$$2d \sin\theta = (m + 1/2)\lambda \quad (2)$$

The following indicates how the complex refractive index (N) has been used to calculate the speed at which electromagnetic waves travel across a material [7]:

$$N = n - ik \quad (3)$$

In this case, n is the real part of the refractive index and k is the extinction coefficient (which represents the imaginary part of the complex refractive index). Additionally, the absorption coefficient (α) is equal to

Vol. 08 No. 1, April-2026, Pages 49-52 DOI: https://dx.doi.org/10.20961/jeeict.8.1.116584

$\alpha=4\pi k/\lambda$, where λ is the incident light's wavelength [8]. The thickness of the layers, the materials employed, their refractive indices, and other parameters all have an impact on this occurrence. As seen in Fig. 2, anti-reflective coatings (ARCs) can be classified according to a number of factors, including the number of layers, which can be single, double, or multilayer designs.

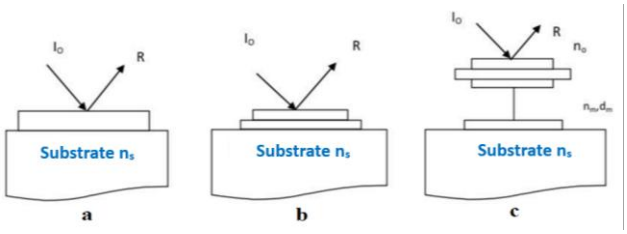

Fig. 2. Coating layer structure of (a) Single layer, (b) Double layer, (c) Multilayer.

II. METHODS

Cadmium sulfide (CdS) and zinc sulfide (ZnS) thin films were fabricated on Corning glass using the ultrasonic spray pyrolysis process. This involved a solution of 0.1 M cadmium chloride ($CdCl_2 \cdot 2H_2O$ with a purity of at least 99%) and zinc chloride ($ZnCl_2$ with a purity of at least 98%), with thiourea taken from Sigma-Aldrich Co., which required no additional purification. Metal salts and thiourea were mixed in a 1:1 ratio with water and vigorously stirred at 30 °C until a clear solution was obtained. Fig. 3 presents multiple components of the spray pyrolysis apparatus. The solution was atomized into fine droplets using a nebulizer and transmitted through a stream of air. Various characterization methods, including Raman spectroscopy, atomic force microscopy (AFM), UV-visible absorbance, and a reflectance probe, were used to characterize the samples, assess reflectance spectra, and determine the thickness of the samples.

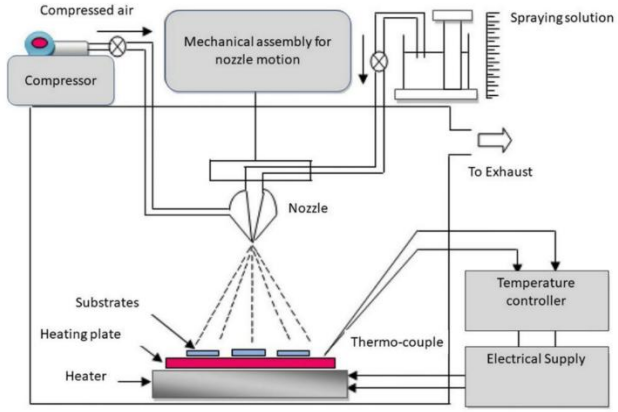

Fig. 3. Schematic of spray pyrolysis technique and its equipment.

III. RESULTS AND DISCUSSION

To measure the thickness of thin films that were deposited for different lengths of time, a reflectance probe was used. After 15 minutes of deposition, the thickness increased gradually, finally reaching 229 nm for ZnS and 291 nm for CdS (Table I).

Figs. 4 and 5 demonstrate the Raman spectra of ZnS and CdS thin films prepared at room temperature through 15 min deposition time, within the wavenumber range 100 to 1600 cm^{-1}. E_1 longitudinal optical (LO) phonon mode centered at 566 cm^{-1} in the Raman spectrum also strongly supports the wurtzite ZnS nature [11]. The band at 1100 is attributed to S anions in the lattice. Bands at 484 and 566 cm^{-1} are attributed to the higher-order combination bands of the fundamental modes [12].

TABLE I. THICKNESS OF ZNS AND CDS THIN FILMS DEPOSITED AT DIFFERENT PERIODS

Deposition time (min)	Thickness (nm)	
	ZnS	*CdS*
5	75	105
10	150	211
15	229	291

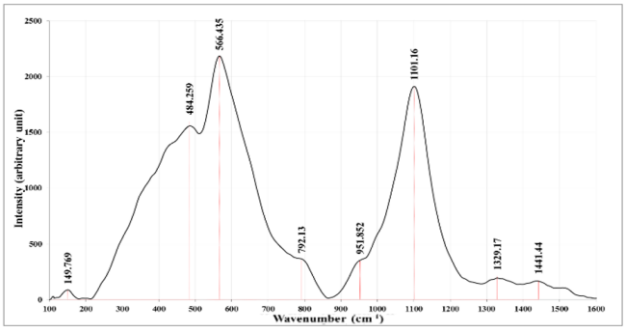

Fig. 4. Raman spectrum of ZnS thin films prepared using 15 min deposition time.

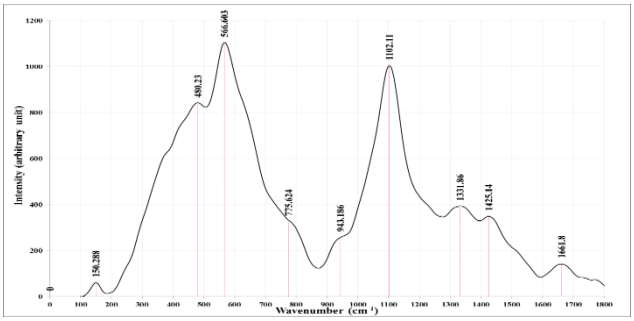

Fig. 5. Raman spectrum of CdS thin films prepared using 15 min deposition time.

AFM images and particle size distribution histograms for ZnS and CdS thin films made by 15 min deposition time are presented in Figs. 6 and 7. The average ZnS grain diameter was 161 nm, compared to CdS 306 nm. The standard deviations of particle size were 148 nm and 173 nm for ZnS and CdS thin films, respectively. These results demonstrate the greater regularity of the ZnS compared to the CdS sample [13].

Figs. 8 and 9 show the absorption curves and Tauc plot to determine the optical bandgap of ZnS and CdS thin films deposited at different periods. The absorption edge appeared at about 350 nm and slightly blue-shifted with increasing deposition time for the two materials. The optical band gap $E_{g,opt}$ was determined using the Tauc analysis (the relation between $(\alpha h\upsilon)^2$ versus $h\upsilon$). The $E_{g,opt}$ was 4.1 eV for the ZnS thin film deposited for 5 min, and reduced to 3.9 eV with increasing deposition time to 15 min. The $E_{g,opt}$ for the CdS thin films deposited for 5 min was 2.6 eV and reduced to 2.3 eV for a deposition time of 15 min. The relatively low absorbance of the two materials in the visible range allows for their exploitation as window layers in solar cell applications [14].

Vol. 08 No. 1, April-2026, Pages 49-52 DOI: https://dx.doi.org/10.20961/jeeict.8.1.116584

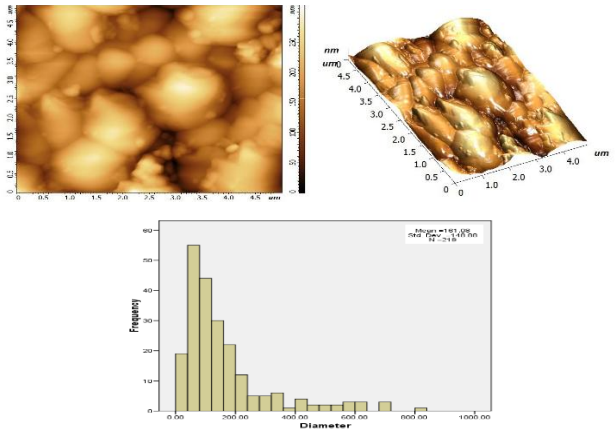

Fig. 6. The 2-D and 3-D AFM images and particle size distribution of ZnS thin films prepared using 15 min deposition time.

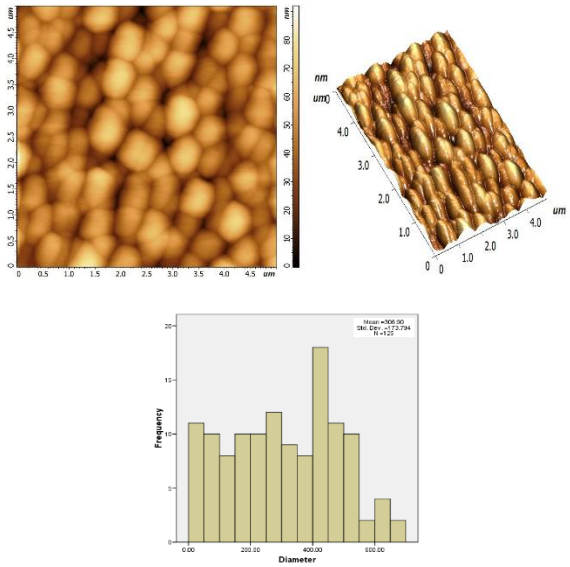

Fig. 7. The 2-D and 3-D AFM images and particle size distribution of CdS thin films prepared using 15 min deposition time.

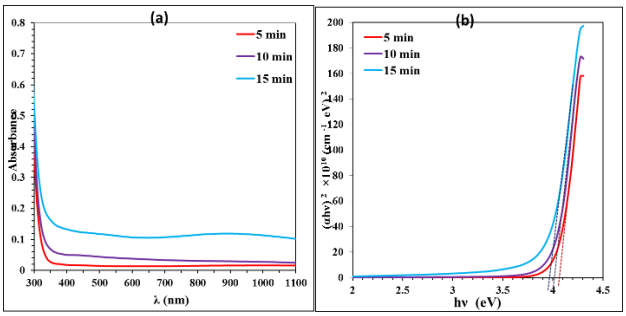

Fig. 8. Absorption curves and Tauc plot $(\alpha h\nu)^2$ vs. hν for ZnS thin films prepared at different times.

The absorbance curves and Tauc plot of the ZnS, CdS, and ZnS/CdS thin films are shown in Fig. 10. At roughly 350 nm, the absorption edge became visible. The optical band gap $E_{g,opt}$ was calculated using the Tauc formula, which is the relationship between $(\alpha h\nu)^2$ and hν. The ZnS, CdS, and ZnS/CdS thin films that were deposited using 15 minutes had $E_{g,opt}$ indices of 4.1, 2.5, and 3.9 eV, respectively.

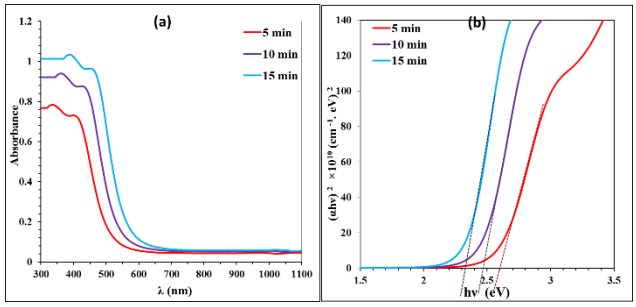

Fig. 9. Absorption curves and Tauc plot $(\alpha h\nu)^2$ vs. hν for CdS thin films prepared at different times.

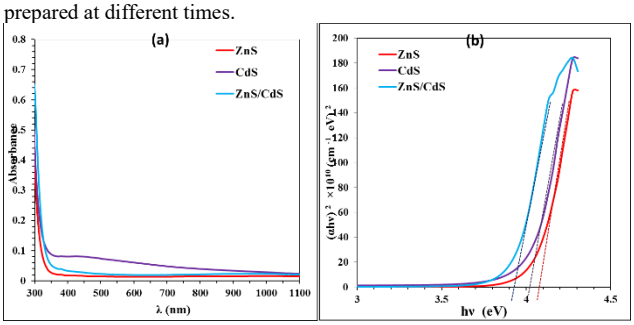

Fig. 10. Absorption curves and Tauc plot (αhν) 2 vs. hν for ZnS, CdS, and ZnS/CdS thin films.

At 15 min deposition, the reflectance curves for the ZnS, CdS, ZnS/CdS thin films are compared (Fig. 11). Thin films with two layers of CdS/ZnS have lower reflectivity than other films. The reflectivity decreases especially in the middle of the solar spectrum at 530 nm, particularly for the double-layered sample.

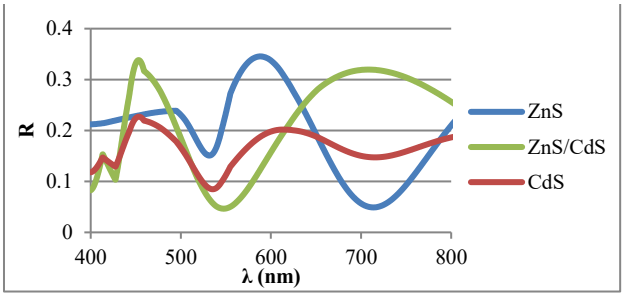

Fig. 11. Reflectance curves for ZnS, CdS, and ZnS/CdS thin films.

IV. Conclusion

Single- and double-layer ZnS-CdS thin films have been successfully deposited on glass substrates under spray pyrolysis with a nebulizer approach as a promising low-cost antireflective coating for high refractive index in the visible range for solar cells. ZnS and CdS thin films are confirmed to form by Raman spectroscopy. The average grain size determined by the AFM analysis was 161 nm for ZnS and 306 nm for CdS. The optical properties show low optical absorbance, with an energy gap of approximately 4.1 eV for the ZnS thin films and ranging from 2.3 to 2.6 eV for the CdS thin films. The reflectivity decreases especially at the middle of the solar spectrum at 530 nm, particularly for the double-layer sample.

Vol. 08 No. 1, April-2026, Pages 49-52 DOI: https://dx.doi.org/10.20961/jeeict.8.1.116584

REFERENCES

[1] J. Nelson, *The Physics of Solar Cells*. London, UK: Imperial College Press, 2003.

[2] D. R. Wright, E. S. Marstein, and A. Holt, "Double layer anti-reflective coatings for silicon solar cells," in *Proc. 31st IEEE Photovoltaic Specialist Conference*, 2005, pp. 1237–1240, doi: 10.1109/PVSC.2005.1488363.

[3] C. J. Brinker and M. S. Harrington, "Sol-gel derived antireflective coatings for silicon," *Solar Energy Materials*, vol. 5, no. 2, pp. 159–172, 1981, doi: 10.1016/0165-1633(81)90027-7.

[4] B. S. Richards, "Single-material TiO_2 double-layer antireflection coatings," *Solar Energy Materials and Solar Cells*, vol. 79, no. 3, pp. 369–390, 2003, doi: 10.1016/S0927-0248(02)00473-7.

[5] P. Vitanov, X. Loozen, A. Harizanova, T. Ivanova, and G. Beaucarne, "A study of sol-gel deposited Al_2O_3 films as passivating coatings for solar cells application," in *Proc. 23rd European Photovoltaic Solar Energy Conference and Exhibition*, Valencia, Spain, 2008, pp. 1596–1599.

[6] Z. Liang, D. Chen, C. Feng, J. Cai, and H. Shen, "Crystalline silicon surface passivation by the negative charge dielectric film," *Physics Procedia*, vol. 18, pp. 51–55, 2011, doi: 10.1016/j.phpro.2011.06.056.

[7] P. K. Biswas *et al*., "Porous anti-reflective silica coatings with high spectral coverage by sol-gel spin coating technique," *Journal of Materials Science Letters*, vol. 22, no. 3, pp. 181–183, 2003, doi: 10.1023/A:1022241707860.

[8] Q. Zhang, J. Wang, G. Wu, J. Shen, and S. Buddhudu, "Interference coating by hydrophobic aerogel-like SiO_2 thin films," *Materials Chemistry and Physics*, vol. 72, no. 1, pp. 56–59, 2001, doi: 10.1016/S0254-0584(01)00322-4.

[9] P. Nostell, A. Roos, and B. Karlsson, "Optical and mechanical properties of sol-gel antireflective films for solar energy applications," *Thin Solid Films*, vol. 351, no. 1–2, pp. 170–175, 1999, doi: 10.1016/S0040-6090(99)00257-6.

[10] A. Gombert *et al*., "Glazing with very high solar transmittance," *Solar Energy*, vol. 62, no. 3, pp. 177–188, 1998, doi: 10.1016/S0038-092X(98)00008-5.

[11] D. R. Uhlmann, T. Suratwala, K. Davidson, J. M. Boulton, and G. Teowee, "Sol-gel derived coatings on glass," *Journal of Non-Crystalline Solids*, vol. 218, pp. 113–122, 1997, doi: 10.1016/S0022-3093(97)00162-2.

[12] C. Zha, X. Luo, R. Wang, and B. L. Davies, "Effects of TiO_2 and ZrO_2 on optical properties of organic–inorganic hybrid polymers and thin films," *Journal of Materials Science: Materials in Electronics*, vol. 18, p. 331, 2007, doi: 10.1007/s10854-007-9216-6.

[13] H. H. Nwe, Y. M. Maung, T. T. Win, and K. K. K. Soe, "Photovoltaic properties of mesoporous TiO_2–ZrO_2 binary oxide electrode with sawdust organic dye for dye-sensitized solar cell application," *Journal of Science*, vol. 3, no. 1, p. 197, 2012.

[14] J. Li *et al*., "Design, preparation, and durability of TiO_2/SiO_2 and ZrO_2/SiO_2 double-layer antireflective coatings in crystalline silicon solar modules," *Solar Energy*, vol. 89, pp. 134–142, 2013, doi: 10.1016/j.solener.2012.12.011.

Vol. 08 No. 1, April-2026, Pages 49-52 DOI: https://dx.doi.org/10.20961/jeeict.8.1.116584